

Wavelet investigation of $\text{La}_{0.5}\text{Ca}_{0.5}\text{CoO}_{3-\delta}$ x-ray absorption data

M. Sahnoun and C. Daul

Department of Chemistry, University of Fribourg, CH-1700 Fribourg, Switzerland

O. Haas^{a)}

Paul Scherrer Institut, CH-5232 Villigen PSI, Switzerland

Morlet wavelet transformation was used to analyze the Co *K*-edge extended x-ray absorption spectrum of $\text{La}_{0.5}\text{Ca}_{0.5}\text{CoO}_{3-\delta}$. Due to recent success in wavelet analysis of extended x-ray absorption fine structure (EXAFS) data we hoped that the Co–La scattering path could be separated from the Co–Ca scattering path in the EXAFS spectrum of $\text{La}_{0.5}\text{Ca}_{0.5}\text{CoO}_{3-\delta}$. The result showed a certain resolution of the wavelet transformed spectrum in the *k* space. Using theoretical scattering functions of the individual scattering paths calculated with *ab initio* multiple scattering codes (FEFF), it was possible to assign some maxima in the wavelet transformation EXAFS spectrum. The Co–La scattering path could be identified, but no additional information about the Co–Ca scattering function was obtained. A detailed analysis of the theoretical Co–La and Co–Ca scattering functions revealed that the two scattering functions overlap considerably in *k* space and have almost the same frequency. Morlet wavelet transformation of the sum of the two theoretical scattering functions did not allow a satisfactory separation of the two scattering functions. This separation is probably only possible with wavelets, which mimic the fundamental properties of the real scattering function more accurately.

I. INTRODUCTION

Fourier transformation (FT) of x-ray absorption fine structure (EXAFS) spectra has been widely used to obtain structural information from x-ray absorption data.¹ However, using FT it is not possible to separate the scattering contributions of nearest neighbor atoms with similar distances. Recently, Funke and co-workers^{2–5} demonstrated with an investigation on Zn–Al layered double hydroxides that it is possible to separate the scattering contributions of nearest neighbor atoms at similar distances but with different atomic numbers using Morlet wavelet transformation. Wavelet transformation (WT) has also been used for other purposes in x-ray absorption spectroscopy. Muñoz *et al.*⁶ showed that it is possible to separate the x-ray appearance near-edge structure (XANES) region (near edge x-ray absorption) from the EXAFS region, and a more sophisticated wavelet analysis of EXAFS data has been published by Yamaguchi *et al.*⁷ using a linear inverse problem algorithm based on the Galerkin wavelet method. They demonstrated that this method allows the evaluation of a more accurate radial structure function even from noisy Cu *K*-edge samples. Due to all these promising results the WT becomes much more popular in analyzing x-ray absorption spectra.

We are interested in the interpretation of the Co *K*-edge x-ray absorption data of $\text{La}_{1-x}\text{Ca}_x\text{CoO}_{3-\delta}$ perovskites. In a previous publication we analyzed x-ray absorption spectra from LaCoO_3 using FT and *ab initio* multiple scattering (FEFF) simulation⁸ and published also some x-ray absorption spectra in connection with an electrochemical investigation of $\text{La}_{1-x}\text{Ca}_x\text{CoO}_{3-\delta}$ perovskites.⁹ Sahnoun *et al.*¹⁰ investi-

gated also the electronic structure of $\text{La}_{1-x}\text{Ca}_x\text{CoO}_{3-\delta}$ ($x = 0, 0.5$) using full potential calculations which is helpful for the interpretation of the XANES region of the $\text{La}_{1-x}\text{Ca}_x\text{CoO}_{3-\delta}$ x-ray absorption spectra.

The present work reports about a wavelet-transformation analysis of the Co *K*-edge EXAFS region of $\text{La}_{0.5}\text{Ca}_{0.5}\text{CoO}_{3-\delta}$ where Morlet wavelets were used to study if it is possible to distinguish between the Co–La and Co–Ca scattering paths. For the interpretation of the Morlet WT the theoretical Co–La and Co–Ca scattering functions of $\text{La}_{0.5}\text{Ca}_{0.5}\text{CoO}_{3-\delta}$ were calculated using the *ab initio* multiple scattering FEFF8.2 code.¹¹

II. BASIC WAVELET ANALYSIS

Wavelet analysis (WA) was first used to analyze signals in the time and frequency domains. Such two dimensional analysis can also be performed using windowed FT. The advantages of the wavelet transformation, however, are the possibility to use other functions than complex conjugated sinus functions as a probe to analyze the signal. The signal can therefore be analyzed with a function (mother wavelets), which resembles the components of the signal. The mother wavelets are the basic wavelets used as kernels for the continuous wavelet transforms (CWTs). They are built from a wide and flexible class L^2 with zero mean,

$$\int_{-\infty}^{+\infty} \Psi(t) dt = 0. \quad (1)$$

This weak condition enables one to find a mother wavelet adapted to almost any field of application. In addition, the wavelet can be scaled. The kernel of the CWT is obtained by translation (parameter *b*) and scaling (parameter *a*) of the

^{a)} Author to whom correspondence should be addressed; FAX: +41-56-310-2199; electronic mail: otto.haas@psi.ch

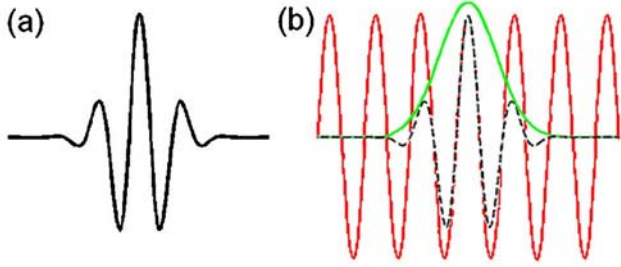


FIG. 1. (Color online) (a) Morlet wavelet corresponding to Morlet parameters $\kappa=5$, $\sigma=1$. (b) Construction of the Morlet wavelet as a sine curve modulated by a Gaussian.

chosen mother wavelet. The WT of a signal $f(t)$ is defined by the following equation:

$$W_f^{\Psi(\kappa,\sigma)}(a,b) = \frac{1}{\sqrt{|a|}} \int_{-\infty}^{\infty} f(t) \Psi_{(\kappa,\sigma)}^* \left(\frac{t-b}{a} \right) dt, \quad (2)$$

where Ψ^* is the complex conjugated function of the wavelet. The combined translation and dilatation of the argument of the mother wavelet can be used to shape the wavelet. It allows the optimal extraction of information of both the time and frequency behaviors of the signal.

The magnitude of the WT has higher values, whenever the wavelet function and the signal function have an overlapping domain, e.g., if the wave number ω of the signal and the wave number of the wavelet are the same in the same period of time [ω is the frequency parameter in $f(t)$ and $\Psi(t)$].

The CWT analysis can be adapted to EXAFS analysis if t is exchanged with k and $2\pi\omega$ with $2r$ to go from the time-frequency regime to the electron wave vector radial distance regime.² To analyze the EXAFS part of an x-ray absorption spectrum the $\chi(k)$ function of the XAS spectrum has to be investigated. In order not to lose the signals at higher k values the spectrum is normally multiplied by k^3 or k^2 . The $\chi(k)k^3$ looks very much like a complex time-frequency signal but with k as a variable instead of t . The CWT of the $\chi(k)k^3$ is thus a function of (k,r) instead of (t,ω) , where r is the phase and amplitude uncorrected radial distance to the scattering atom (or scattering shell).

The expression of the CWT of the k^3 -weighted EXAFS data can be written as follows:

$$W_{\chi}^{\Psi(\kappa,\sigma)}(k,r) = \sqrt{2r} \int_{-\infty}^{+\infty} \chi(k') k'^3 \Psi_{(\kappa,\sigma)}^* [2r(k'-k)] dk', \quad (3)$$

where $\chi(k)$ function is the measured EXAFS function, k the electron wave vector, and $\Psi_{(\kappa,\sigma)}$ is the wavelet which includes a periodic function multiplied by a bell-shaped function, which attenuates the amplitude to zero outside the window. To analyze EXAFS data, the Morlet wavelets¹² (see Fig. 1) have some advantages. First, the structure of the Morlet wavelet is rather similar to the $\chi(k)k^3$. Second, the formal mathematical description of the wavelet analysis can be treated in analogy to the Fourier analysis.

The Morlet wavelet shown in Fig. 1(a) is defined as the product of a complex exponential wave and a Gaussian envelope:

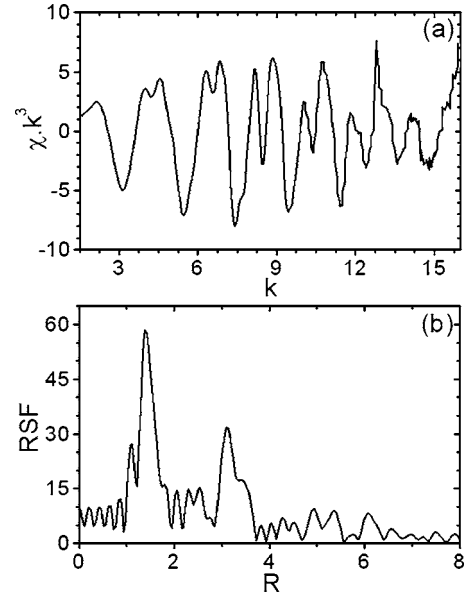


FIG. 2. (a) $\chi(k)k^3$ of the experimental $\text{La}_{0.5}\text{Ca}_{0.5}\text{CoO}_{3-\delta}$ Co K-edge spectrum. (b) Radial structure function of $\text{La}_{0.5}\text{Ca}_{0.5}\text{CoO}_{3-\delta}$ [Fourier transform of $\chi(k)k^3$].

$$\psi_0(k) = \frac{1}{\sqrt{2\pi\sigma}} [e^{i\kappa k} - e^{-\kappa^2/2}] e^{-k^2/2\sigma^2}, \quad (4)$$

where ψ is the wavelet value at the wave vector k , σ is the “dilation” parameter used to change the scale, and κ is the frequency of the sine and cosine functions. It is a free wavelet parameter which indicates how much oscillations of the sine wave are covered by a Gaussian envelope with the half-width $\sigma=1$. Using scaled wavelets allows us to adapt the wavelet to the problem to be investigated.

III. DATA TREATMENTS

XAS data. The reduction of the x-ray absorption data was performed with the software program WINXAS (Ref. 13) using standard procedures for energy calibration background correction, normalization E_0 , determination and transformation in the k space. We used a cubic spline fit to deduce the atomic x-ray absorption spectrum from the molecular spectrum to generate the $\chi(k)$ function. The resulting $\chi(k)$ function was weighted with k^3 to account for weakening of oscillation amplitudes with increasing k . The so obtained $\chi(k)k^3$ function [see Fig. 2(a)] was then used for the FT and the WT.

Fourier transformation. To generate the radial structure function [see Fig. 2(b)] the $\chi(k)k^3$ function [Fig. 2(a)] was Fourier transformed in a limited k range, while applying a window based on Bessel functions with a smoothening parameter of 3 to diminish artifacts due to the finite Fourier filtering range. We used a k range (1.5–16.0) which allowed a transformation with no unexpected peaks below reasonable atomic distances.

Wavelet transformation. Morlet wavelets were used for the WT of the experimental $\chi(k)k^3$ signal (see Fig. 3) and of the theoretical FEFF functions (see Figs. 4 and 6), where the FORTRAN program HAMA (Ref. 2) together with ORIGINIAB

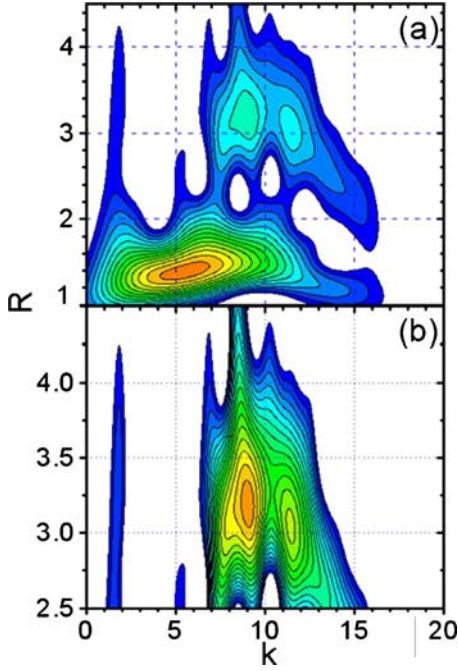


FIG. 3. (Color online) Morlet WT of the experimental $\chi(k)k^3$ of $\text{La}_{0.5}\text{Ca}_{0.5}\text{CoO}_{3-\delta}$ using $\kappa=5$ and $\sigma=1$.

software were used to calculate and visualize the wavelet transformation.

IV. FEFF FILE GENERATION

The contribution of individual scattering path to the $\chi(k)$ function¹⁴ of an EXAFS spectrum was calculated using the FEFF8.2 code^{11,15} and the atomic positions in the unit cell.¹⁶ FEFF codes developed by Rehr and co-workers^{11,15,17} calculate EXAFS functions and individual scattering path functions using an *ab initio* self-consistent real space multiple scattering approach for clusters of atoms. The sum of all possible FEFF files (scattering paths) leads to a theoretical EXAFS spectrum [$\chi(k)$ function]. At low temperature the cobalt is in the low spin state, and LaCoO_3 and $\text{La}_{0.5}\text{Ca}_{0.5}\text{CoO}_{3-\delta}$ prefer the cubic $Pm\bar{3}m$ space group symmetry at room temperature; the structure shows a slight rhombohedral distortion. To calculate the FEFF input file we used the cubic atomic positions for LaCoO_3 as listed in Table I, but changed in the FEFF input file every second La by Ca. This FEFF input file was then used to generate the FEFF files with phases and amplitudes for each scattering path using the FEFF8.2 code. All possible scattering paths for $\text{La}_{0.5}\text{Ca}_{0.5}\text{CoO}_{3-\delta}$ up to 4.5 Å are listed in Table II, where the paths, which we would like to separate by WT, are highlighted. The theoretical scattering function of the Co–La and Co–Ca paths in the EXAFS spectrum of $\text{La}_{0.5}\text{Ca}_{0.5}\text{CoO}_3$ is shown in Fig. 4 and the sum of the Co–La and Co–Ca scattering functions in Fig. 5(b).

V. DISCUSSION

Figure 2(a) shows the experimental $\chi(k)k^3$ signal of $\text{La}_{0.5}\text{Ca}_{0.5}\text{CoO}_{3-\delta}$ and Fig. 2(b) the radial structure function [FT of $\chi(k)k^3$]. The radial structure function shows a domi-

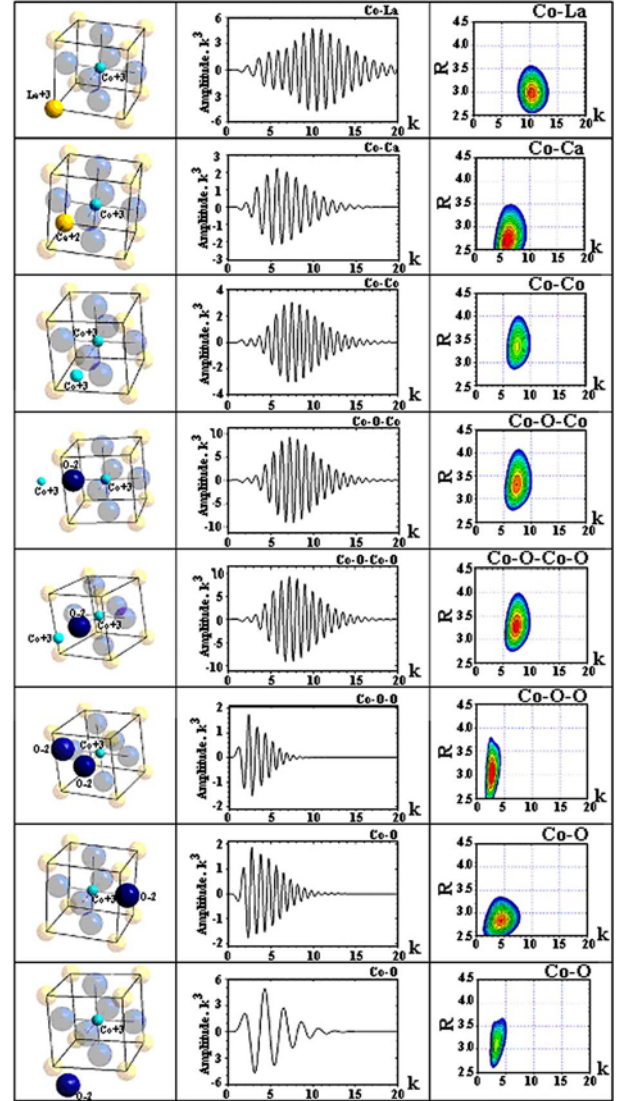


FIG. 4. (Color online) Left column illustration of the scattering path, middle column scattering path functions times k^3 , right column Morlet WT of the scattering functions times k^3 using the Morlet parameters $\kappa=5$, $\sigma=1$.

nant peak at $R=1.5$ Å and at $R=3.1$ Å, where R stands for the phase and amplitude not corrected radius of the scattering shells around the x-ray absorbing central Co atom. The first peak is due to the Co–O scattering path, whereas the second dominant peak at about $R=3$ and the intermediate peak at about $R=2.4$ contain scattering contributions of several scattering paths, e.g., Co–La, Co–Ca, Co–Co, and several multiple scattering contributions as can be seen from Table II [N.B. r_{eff} are the effective radii of the atomic shells around Co and are about 0.5 Å larger than the phase and amplitude of not

TABLE I. Positions of the atoms of LaCoO_3 based on $Pm\bar{3}m$ (221) space group symmetry with unit cell lengths $a=b=c=3.82$ Å and angles $\alpha=\beta=\gamma=90^\circ$ (Ref. 16). M=Multiplicity; Wy=Wyckoff notation.

Atom	M	(Wy)	X	Y	Z
La	1	(a)	0.0	0.0	0.0
Co	1	(b)	0.5	0.5	0.5
O	3	(c)	0.5	0.5	0.0

TABLE II. List of all FEFF files of $\text{La}_{0.5}\text{Ca}_{0.5}\text{CoO}_{3-\delta}$ in the scattering range $r=1.9-4.5$ Å.

File	Sigma ²	Amp. ratio	deg	Nleg	r_{eff}	Scattering path
feff0001.dat	0.0056	100.00	6	2	1.910	Co-O (180°, 180°)
feff0002.dat	0.0094	16.90	24	3	3.261	Co-O-O (90°,135°, 135°)
feff0003.dat	0.0022	30.57	4	2	3.308	Co-La (180°, 180°)
feff0004.dat	0.0038	23.10	4	2	3.308	Co-Ca (180°, 180°)
feff0005.dat	0.0030	21.45	6	2	3.820	Co-Co (180°, 180°)
feff0006.dat	0.0112	16.43	6	3	3.820	Co-O-O (0°,180°, 180°)
feff0007.dat	0.0030	58.80	12	3	3.820	Co-Co-O (180°,180°, 0°)
feff0008.dat	0.0112	12.22	6	4	3.820	Co-O-Co-O (0°,180°, 0°, 180°)
feff0009.dat	0.0022	5.74	6	4	3.820	Co-O-Co-O (180°, 180°, 180°,180°)
feff0010.dat	0.0030	40.70	6	4	3.820	Co-O-Co-O (180°, 0°, 180°, 0°)
feff0012.dat	0.0043	8.25	24	3	3.960	Co-La-O (125°, 145°, 90°)
feff0013.dat	0.0057	7.43	24	3	3.960	Co-Ca-O (125°, 145°, 90°)
feff0014.dat	0.0070	57.33	24	2	4.271	Co-O (180°, 180°)
feff0015.dat	0.0075	53.92	48	3	4.441	Co-O-O (153°, 162°, 45°)

corrected R values obtained from the radial structure function shown in Fig. 2(b)]. There are seven principal scattering paths with a relative intensity of more than 20% in the range $r_{\text{eff}}=2-4.5$. The maxima of the scattering amplitudes of individual scattering paths appear normally at different k values. Scattering atoms with low atomic numbers have a prominent appearance at low k , whereas scattering atoms with high atomic numbers have their maximum amplitude at higher k values. This allows the separation of scattering paths using wavelet transformation. However, not all scattering paths have their amplitude maximum at very different values and the scattering functions overlap normally quite a bit which is not favorable for a good separation by WT. Figures 3(a) and 3(b) show the result of WT of the experimental $\chi(k)k^3$. The Co-O scattering path is easily separated from the other scattering paths but it shows a maximum at $R=1.4$ and $k=5.5$. The separation of the first atomic shell from the other shells is also possible with a simple FT, as can be seen in Fig. 2(b). Our interest in WT is the r_{eff} range

between 2.5 and 4.5 Å (or $R=2-4$ Å), where the Co-La and the Co-Ca scattering paths should be included. This region shows a maximum at $k=9$ with a shoulder at $k=8$ and a second prominent maximum at $k=11.5$. In addition, it has a weaker maximum at $k=2$, which is not sharp in R . The interpretation of this result is difficult without additional information. Useful hints can be obtained from theoretical scattering path simulation using FEFF codes. In Table II, all possible scattering paths in the range $r=1.9-4.5$ are listed. It shows that the scattering paths we are interested in (Co-La and Co-Ca) have unfortunately only weak intensities and the EXAFS signal is rather dominated by several multiple scattering paths.

Figure 4 shows the results of calculations of the most important scattering functions and their WT. In the first column the scattering path is illustrated, where the scattering atoms involved in the $\text{La}_{0.5}\text{Ca}_{0.5}\text{CoO}_3$ perovskite are highlighted and tagged. The second column shows the scattering functions times k^3 of the scattering paths calculated with FEFF8.2. The third column shows the wavelet transformed scattering functions times k^3 .

Comparing the positions of the maxima of the wavelet transformed scattering functions times k^3 with the maxima of the wavelet transformed experimental $\chi(k)k^3$ function, we assign the maximum at $k=11.5$ in Fig. 3 to the Co-La scattering path, and the maximum at $k=2$ to the multiple scattering path Co-O-O as well as to the second shell Co-O scattering path. The more structured and broader maximum at $k=9$ may be a superposition of Co-Ca, Co-Co, and Co-O-Co-O.

Due to the fact that the Co-La scattering function has its maximum at relative high k values, it seems possible to separate the Co-La scattering path from a whole bunch of other scattering paths of the second scattering shell in the perovskite, which offers the possibility to analyze this scattering paths separately.

However, it is not sure if the Co-Ca scattering path is really separated from the Co-La scattering path. The Co-Ca scattering function times k^3 is strongly overlapping with the Co-La scattering function times k^3 (see Fig. 5). In addition,

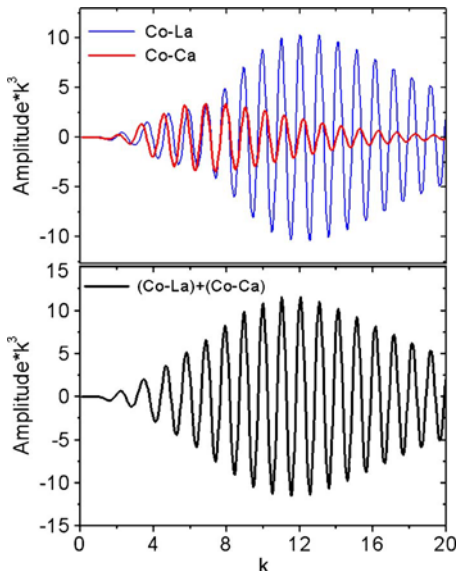


FIG. 5. (Color online) Scattering function times k^3 of Co-La and Co-Ca and sum of the two functions.

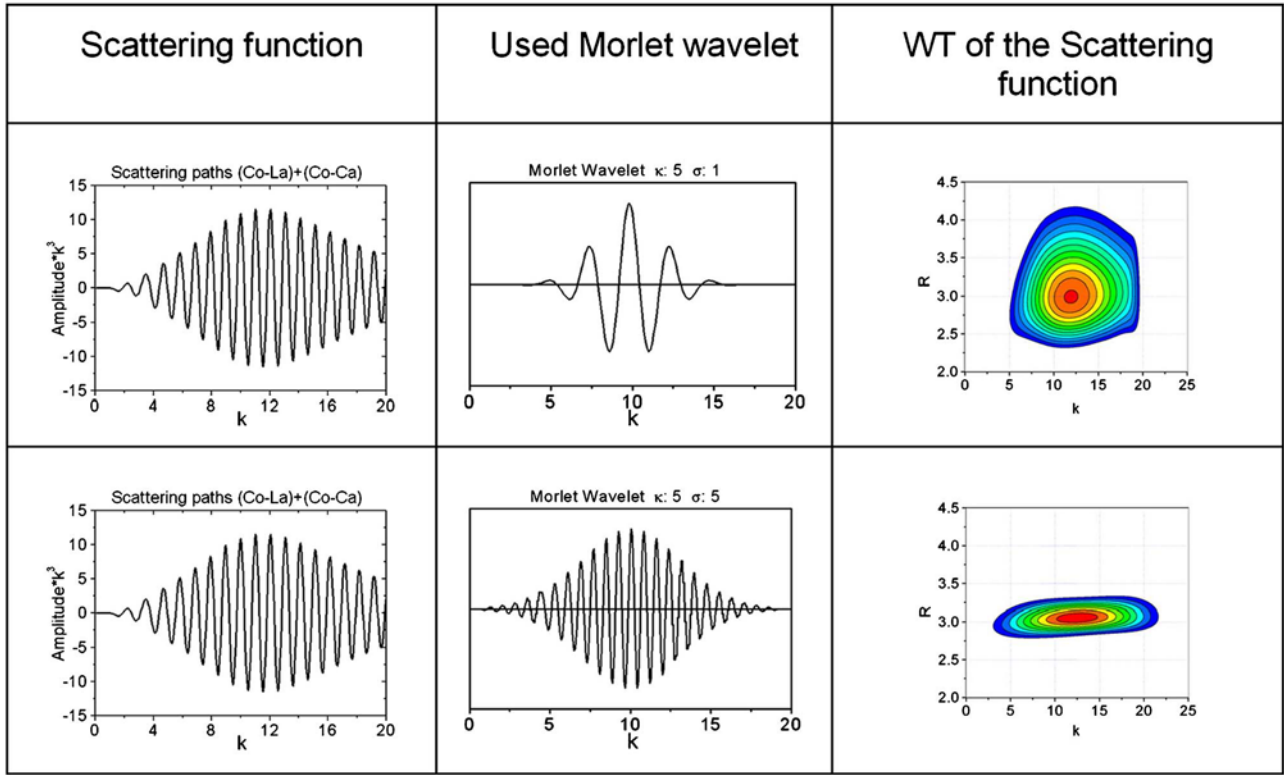


FIG. 6. (Color online) Morlet WT of the sum of the two scattering functions shown in Fig. 5 using two different Morlet parameters (a) $\kappa=5$, $\sigma=1$; (b) $\kappa=5$, $\sigma=5$.

these two functions have the same frequency (same r_{eff}) and differ only in the phase; the two functions may mix to a function which is not separable by a Morlet wavelet transformation.

To answer the question if the Co–La scattering path can be separated from the Co–Ca scattering path the sum of the two theoretical scattering functions times k^3 was wavelet transformed as illustrated in Fig. 6. It can be seen from Fig. 6 that a clean separation between the two scattering functions is not possible; using Morlet wavelets with $\kappa=5$ and $\sigma=1$ there is no separation at all. Due to the fact that the signals of the two scattering paths are so large, a broader wavelet with an appearance closer to the signal was used for the transformation shown in the second column of Fig. 6. Such a wavelet can, e.g., be obtained if $\kappa=5$ and $\sigma=5$ are used as wavelet parameters. Figure 6 shows that this wavelet allows the determination of much more accurate r values. The signal is somehow tailed but it still does not allow an unambiguous separation of the two scattering paths. Comparing the WT of the sum of the two scattering functions (Fig. 6) with the WT of the individual Co–La and Co–Ca scattering functions depicted in Fig. 4, we recognize that the two individual scattering functions have their maxima at slightly different R values. This is also the case if the two functions are Fourier transformed. At a first glance, this may surprise since we know that they have the same r_{eff} value, but this can be explained by the fact that the two functions have the same frequency but not the same phase (k) and amplitude (k) functions.

Although the Morlet wavelets may be useful for special cases in the analysis of EXAFS data, they have some short-

comings if the scattering functions are strongly overlapping each other with similar frequencies. Even though the maxima of the scattering functions times k^3 are located at different k values, the two functions cannot be separated satisfactorily using Morlet wavelets. Better separation could probably be achieved if the wavelet would be better adapted to the shape and the phase properties of the scattering functions. EXAFS signal has characteristic k dependency of the phase shift and the backscattering amplitude which depends on the absorbing and scattering atom.¹⁸ This property cannot be probed with a simple Morlet wavelet. The best wavelet would probably be a wavelet constructed out of the EXAFS function.

VI. CONCLUSIONS

In many cases Morlet WT of EXAFS data may have some advantages compared to traditional FT of EXAFS data since it provides not only radial distance resolution but also resolution in k space. Atoms with similar radial distances but different atomic numbers may be treated separately after resolving in k space. In the case of Co K -edge EXAFS spectrum of $\text{La}_{0.5}\text{Ca}_{0.5}\text{CoO}_{3-\delta}$, it would be of interest to separate the scattering contribution of the Co–La and Co–Ca scattering paths. The wavelet investigation of the Co K -edge EXAFS spectrum of $\text{La}_{0.5}\text{Ca}_{0.5}\text{CoO}_{3-\delta}$ pretends that the Co–La scattering path can be separated from the other scattering paths, which is not possible with a data analysis using Fourier transformation alone. A closer look, however, using FEFF code simulated scattering functions, reveals that the Co–La scattering path cannot be separated from the Co–Ca scattering path using Morlet WT due to strong overlapping of the

signal with very similar frequency. More success to separate these functions by WT is expected with wavelets having properties closer to real scattering functions.

ACKNOWLEDGMENT

One of the authors (M.S.) would like to thank the Energy Research Department of the Paul Scherrer Institut for financial support.

¹E. A. Stern, Phys. Rev. B **10**, 3027 (1974).

²H. Funke, A. C. Scheinost, and M. Chukalina, Phys. Rev. B **71**, 094110 (2005).

³H. Funke and M. Chukalina, Research Center Rossendorf Report No. FZR-343, 2001 (unpublished); FZR-373, 2002 (unpublished); FZR-400, 2003 (unpublished); FZR-400, 2003 (unpublished).

⁴H. Funke, M. Chukalina, and A. Rossberg, Phys. Scr., T **115**, 232 (2005).

⁵M. Chukalina, H. Funke, and Y. Dubrovskij, Low Temp. Phys. **30**, 1235 (2004).

⁶M. Muñoz, P. Argoul, and F. Farges, Am. Mineral. **88**, 694 (2003).

⁷K. Yamaguchi, Y. Ito, T. Mukoyama, M. Takahashi, and S. Emura, J. Phys.

B **32**, 1393 (1999).

⁸O. Haas, R. P. W. J. Struis, and J. M. McBreen, J. Solid State Chem. **177**, 1000 (2004).

⁹O. Haas, F. Holzer, S. Müller, J. M. McBreen, X. Q. Yang, X. Sun, and M. Balasubramanian, Electrochim. Acta **47**, 3211 (2002).

¹⁰M. Sahnoun, C. Daul, O. Haas, and A. Wokaun, J. Phys.: Condens. Matter **17**, 7995 (2005).

¹¹A. L. Ankudinov, B. Ravel, J. J. Rehr, and S. D. Conradson, Phys. Rev. B **58**, 7565 (1998).

¹²P. Goupillaud, A. Grossmann, and J. Morlet, Geoeexploration **23**, 85 (1984).

¹³T. Ressler, J. Synchrotron Radiat. **5**, 118 (1998).

¹⁴The $\chi(k)$ function is the characteristic oscillation on top of the atomic XAS spectrum, which reflects the interference of the outgoing electron with the nearest neighbor atoms of the investigated molecule. It is normally investigated as a function of the k vector, where the k vector is the wave number per angstrom of the outgoing electron in the XAS experiment.

¹⁵A. L. Ankudinov, C. E. Bouldin, J. J. Rehr, J. Sims, and H. Hung, Phys. Rev. B **65**, 104107 (2002).

¹⁶A. Wold and R. Ward, J. Am. Chem. Soc. **76**, 1029 (1954).

¹⁷J. J. Rehr and R. C. Albers, Phys. Rev. B **41**, 8139 (1990).

¹⁸B. K. Teo and P. A. Lee, J. Am. Chem. Soc. **101**, 2815 (1979).